J|A|C|S COMMUNICATIONS

Published on Web 01/08/2009

Helical Nanocomposites from Chiral Block Copolymer Templates

Wen-Hsien Tseng,[†] Chun-Ku Chen,[†] Yeo-Wan Chiang,[†] Rong-Ming Ho,*[,†] Satoshi Akasaka,[‡] and Hirokazu Hasegawa[‡]

Department of Chemical Engineering, National Tsing Hua University, Hsinchu 30013, Taiwan, and Department of Polymer Chemistry, Graduate School of Engineering, Kyoto University, Nishikyo-ku, Kyoto, 615-8510, Japan

Received October 14, 2008; E-mail: rmho@mx.nthu.edu.tw

The nanocomposites formed by inorganic and polymeric materials have intense potential to be the candidates for next-generation materials owing to their excellent material properties such as optical, electrical, optoelectronic, mechanical, and magnetic properties. The ability to control the geometries of inorganic nanomaterials (e.g., shape, size, interdistance, and arrangement) in such nanocomposites is the critical issue to justify the performances of the materials. By taking advantage of the self-assembly of block coplymers (BCPs),[1] well-defined nanocomposites can be prepared through the hybridization of inorganic nanoparticles/BCPs[2−5] and of inorganic precursors/BCPs[6−8] as well as loading inorganic nanomaterials into BCP templates.[9] Inorganic helical nanostructures have drawn intense attention because of their applications in nanomechanical, sensing, electronic, electromagnetic, and optoelectronic devices.[10,11] Also, well-oriented inorganic helical nanostructures can be used as photonic crystals,[12] alignment films for liquid crystal displays,[13] and so on. A variety of approaches for the manufacture of inorganic helical nanostructures have been well demonstrated, such as chemical vapor deposition,[10] vapor-solid growth process,[11] glancing angle deposition (GLAD),[14] self-assembly of chiral surfactant/inorganic precursors,[15] and self-assembly of inorganic precursors/achiral surfactant under nanoconfinement.[16] Nevertheless, the formation of well-oriented helical nanostructures remains challenging.

Recently, a novel helical phase was found in the self-assembly of a diblock copolymer system containing both achiral and chiral blocks, poly(styrene)-*b*-poly(L-lactide) (PS-PLLA). The formation of the helical phase is attributed to the contribution of chiral entity. This diblock copolymer system was thus named as chiral block copolymer (BCP*).[17] Well-oriented, hexagonally packed nanohelices of PLLA in the PS matrix could be formed in the self-assembly of the PS-PLLA BCP*.[17] BCPs with aliphatic polyester blocks such as polylactides draw extensive attention in the preparation of nanoporous polymers because the polyesters can be selectively degraded, particularly by hydrolysis.[18] Sol−gel chemistry is a well-known method to synthesize various ceramic oxide compounds.[19]

In this study, with the combination of the self-assembly of degradable BCP* and sol−gel chemistry, three-dimensional ordered helical nanocomposites can be prepared. PS with helical nanochannels is prepared first from the self-assembly of the PS-PLLA BCP* after hydrolysis, and then used as template, as illustrated in Figure 1. By exploiting the nanoreactor concept, sol−gel reaction is then carried out within the template so as to fabricate helical nanocomposites.

Bulk samples of the PS-PLLA BCP* were prepared by solution casting. After quenching from the microphase-separated ordered melt, the thermally treated BCP* were subsequently sectioned by ultramicrotome for transmission electron microscopy (TEM) observation. Figure 2a shows the projection image of the microsection. Because of RuO_4 staining, the PS microdomains appear dark, whereas the PLLA microdomains appear bright. As expected,[17a,b] the projection image suggests the formation of a helical phase. Figure 3a shows the corresponding one-dimensional (1D) SAXS profile of the PS-PLLA bulk samples, and the diffraction peaks are found to occur at q^* ratios of $1:\sqrt{4}:\sqrt{7}:\sqrt{13}$, indicating that those nanohelices are hexagonally packed. The interdomain spacing (i.e., *d*-spacing) was determined as ca. 40.8 nm according to the primary reflection, and the domain size of the nanohelices was estimated to be ca. 18.0 nm from the TEM results.

Subsequently, the PLLA blocks of the PS-PLLA bulk samples were removed by hydrolysis.[17,18] Field emission scanning electron microscopy (FESEM) results demonstrate the formation of the helical nanochannels in the PS matrix (the results are similar to Figure 3 in ref 17a). Figure 3b shows the 1D SAXS profile of the PS-PLLA samples after hydrolysis, at which the diffraction peaks occur at q^* ratios of $1:\sqrt{4}:\sqrt{7}:\sqrt{9}:\sqrt{13}:\sqrt{16}:\sqrt{21}:\sqrt{28}$. The dif-

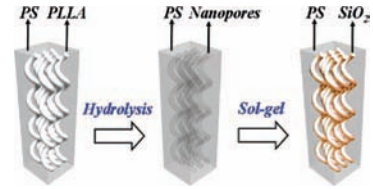

Figure 1. Schematic illustration of the templation for generating well-defined helical nanocomposites.

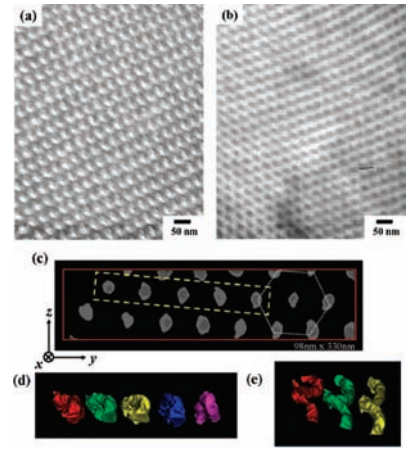

Figure 2. The TEM images of (a) RuO_4 staining PS-PLLA helical nanostructures; (b) PS/SiO_2 helical nanocomposites without staining. The 3D TEM visualization (here the PS phase is transparent): (c) a cross-section sliced view after binarization; images after binarization and segmentation (the domains in the yellow dashed line box in panel c) viewing (d) along and (e) slightly tilt from helical central axes.

[†] National Tsing Hua University.
[‡] Kyoto University.

10.1021/ja808092v CCC: $40.75 © 2009 American Chemical Society

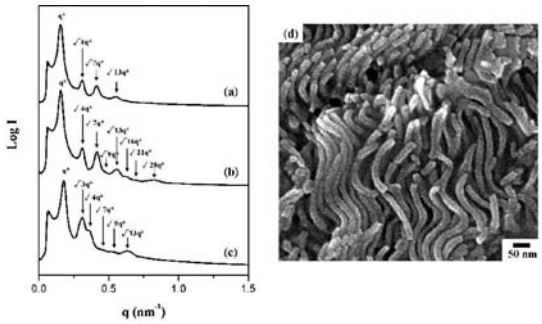

Figure 3. One-dimensional (1D) SAXS profiles of (a) PS-PLLA after quenching from the microphase-separated ordered melt; (b) PS-PLLA after removing PLLA blocks by hydrolysis; (c) PS/SiO_2 helical nanocomposites. (d) The FESEM micrograph of SiO_2 nanohelices from the PS/SiO_2 helical nanocomposites after the treatment of UV exposure.

fraction result is similar to the result of PS-PLLA before removing PLLA blocks (Figure 3a) and the interdomain spacing remains as 40.8 nm, indicating the preservation of the microphase-separated nanostructure after hydrolysis. Also, the significant enhancement on the scattering contrast leads to the appearance of high order reflections so as to further confirm the completion of PLLA hydrolysis. Conversely, PS with hexagonally packed helical nanochannels could be fabricated, and treated as templates for the following sol−gel process (see SI for details). Finally, PS/SiO_2 helical nanocomposite samples can be prepared. Figure 2b displays the projection image of the PS/SiO_2 microsection without RuO_4 staining. In contrast to Figure 2a, similar projection image can be observed. However, it is noted that the contrast is inversed because the PLLA blocks are removed completely by hydrolysis and the SiO_2 is loaded successfully by sol−gel process (see Figure S1 of SI for the projection images viewing at different tilting angles).

Figure 3c shows the corresponding 1D SAXS profile of the PS/SiO_2 helical nanocomposites, at which the diffraction peaks occur at q^* ratios of $1:\sqrt{3}:\sqrt{4}:\sqrt{7}:\sqrt{9}:\sqrt{13}$. Consequently, well-defined hexagonally packed SiO_2 nanohelices in PS matrix can be obtained by carrying out sol−gel reaction within the helical nanochannels (i.e., templation). Nevertheless, the interdomain spacing is reduced to ca. 35.9 nm as compared to the original value of 40.8 nm for the PS templates; it is about 12% reduction in the interdomain spacing after the sol−gel reaction. In comparison of the domain sizes of the PLLA nanohelices and the SiO_2 nanohelices from TEM observation, no significant dimension change can be found. We speculate that the change in the interdomain spacing is caused by the relaxation of helical textures resulting from the swelling of the PS matrix by the sol so as to lead the dimensional change after the formation of dry gel. To further confirm the texture of the templated SiO_2 nanohelices, electron tomography (i.e., 3D TEM) experiments were carried out. As shown in Figure 2, the results clearly show the preservation of the nanohelical texture after the templated sol−gel reaction; hexagonally packed SiO_2 nanohelices can be clearly observed through 3D direct visualization (Figure 2 panels c and d) so as to confirm the hexagonal-cylinder-like character inferring from scattering results. Also, well-defined SiO_2 nanohelices with regular pitch can be clearly recognized in the PS/SiO_2 helical nanocomposites (Figure 2e). It is also noted that the PS/SiO_2 helical nanocomposites could be degenerated by the treatment of UV exposure. The degeneration process was conducted under atmosphere condition for 24 h with a UV source (wavelength = 254 nm and intensity = 3 mW/cm^2). As shown in Figure 3d, the texture of the SiO_2 nanohelices can be clearly visualized after the degeneration of the PS template. Consistent to the TEM results, the domain size of the SiO_2 nanohelices is about 18 nm in average; suggesting the preservation of the nanohelical texture from templation.

In conclusion, we demonstrated the feasibility of nanoreactor concept through the templation of nanoporous PS from degradable BCP* (PS-PLLA) for the fabrication of PS/SiO_2 helical nanocomposites and SiO_2 nanohelices via sol−gel process. In contrast to the varieties of approaches for the preparation of inorganic helical nano-objects, the inorganic nanohelices from the templation of porous nanostructures may provide another dimension for the applications of the helical nanostructures at which well-defined hybridized nanocomposites with ordered texture can be obtained.

Acknowledgment. We thank Prof. Dr. Benjamin S. Hsiao of the Chemistry Department, State University of New York at Stony Brook, and Dr. Lixia Rong of the National Synchrotron Light Source at Brookhaven National Laboratory for their help in synchrotron SAXS experiments. This work is supported by National Science Council (NSC 97-2120-M-007-013).

Supporting Information Available: Characterization of the PS-PLLA BCP*, TEM projection images of helical nanocomposite viewed at different tilting angles. This material is available free of charge via the Internet at http://pubs.acs.org.

References

(1) Bates, F. S.; Fredrickson, G. H. *Annu. Rev. Phys. Chem.* **1990**, *41*, 525–557.
(2) Bockstaller, M. R.; Lapetnikov, Y.; Margel, S.; Thomas, E. L. *J. Am. Chem. Soc.* **2003**, *125*, 5276–5277.
(3) Kim, B. J.; Chiu, J. J.; Yi, G.; Pine, D. J.; Kramer, E. J. *Adv. Mater.* **2005**, *17*, 2618–2622.
(4) Huang, C. M.; Wei, K. H.; Jeng, U. S.; Liang, K. S. *Macromolecules* **2007**, *40*, 5067–5074.
(5) Lo, C. T.; Lee, B.; Pol, V. G.; Rago, N. L. D.; Seifert, S.; Winans, R. E.; Thiyagarajan, P. *Macromolecules* **2007**, *40*, 8302–8310.
(6) Adachi, M.; Okumura, A.; Sivaniah, E.; Hashimoto, T. *Macromolecules* **2006**, *39*, 7352–7357.
(7) (a) Ho, R.-M.; Lin, T.; Jhong, M.-R.; Chung, T.-M.; Ko, B.-T.; Chen, Y.-C. *Macromolecules* **2005**, *38*, 8607–8610. (b) Lo, K.-H.; Tseng, W.-H.; Ho, R.-M. *Macromolecules* **2007**, *40*, 2621–2624.
(8) Lee, D. H.; Kim, H. Y.; Kim, J. K.; Huh, J.; Ryu, D. Y. *Macromolecules* **2006**, *39*, 2027–2030.
(9) Misner, M. J.; Skaff, H.; Emrick, T.; Russell, T. P. *Adv. Mater.* **2003**, *15*, 221–224.
(10) (a) Zhang, H. F.; Wang, C. M.; Wang, L. S. *Nano Lett.* **2002**, *2*, 941–944. (b) Zhang, H. F.; Wang, C. M.; Buck, E. C.; Wang, L. S. *Nano Lett.* **2003**, *3*, 577–580.
(11) (a) Kong, X. Y.; Wang, Z. L. *Nano Lett.* **2003**, *3*, 1625–1631. (b) Kong, X. Y.; Ding, Y.; Yang, R.; Wang, Z. L. *Science* **2004**, *303*, 1348–1351. (c) Gao, P. X.; Ding, Y.; Mai, W.; Hughes, W. L.; Lao, C.; Wang, Z. L. *Science* **2005**, *309*, 1700–1704.
(12) Thiel, M.; Decker, M.; Deubel, M.; Wegener, M.; Linden, S.; Freymann, G. *Adv. Mater.* **2007**, *19*, 207–210.
(13) Sit, J. C.; Broer, D. J.; Brett, M. J. *Adv. Mater.* **2000**, *12*, 371–373.
(14) Robbie, K.; Brett, M. J. *J. Vac. Sci. Technol. A* **1997**, *15*, 1460–1465.
(15) Jin, H.; Liu, Z.; Ohsuna, T.; Ohsuna, T.; Inoue, Y.; Sakamoto, K.; Nakanishi, T.; Ariga, K.; Che, S. *Adv. Mater.* **2006**, *18*, 593–596.
(16) (a) Wu, Y.; Cheng, G.; Katsov, K.; Sides, S. W.; Wang, J.; Tang, J.; Fredrickson, G. H.; Moskovits, M.; Stucky, G. D. *Nat. Mater.* **2004**, *3*, 816–822. (b) Wu, Y.; Livneh, T.; Zhang, Y. X.; Cheng, G.; Wang, J.; Tang, J.; Moskovits, M.; Stucky, G. D. *Nano Lett.* **2004**, *4*, 2337–2342.
(17) (a) Ho, R.-M.; Chiang, Y.-W.; Tsai, C.-C.; Lin, C.-C.; Ko, B.-T.; Huang, B.-H. *J. Am. Chem. Soc.* **2004**, *126*, 2704–2705. (b) Chiang, Y.-W.; Ho, R.-M.; Ko, B.-T.; Lin, C.-C. *Angew. Chem., Int. Ed.* **2005**, *44*, 7969–7972. (c) Ho, R.-M.; Chen, C.-K.; Chiang, Y.-W.; Ko, B.-T.; Lin, C.-C. *Adv. Mater.* **2006**, *18*, 2355–2358.
(18) (a) Zalusky, A. S.; Olayo-Valles, R.; Taylor, C. J.; Hillmyer, M. A. *J. Am. Chem. Soc.* **2001**, *123*, 1519–1520. (b) Tseng, Y.-T.; Tseng, W.-H.; Lin, C.-H.; Ho, R.-M. *Adv. Mater.* **2007**, *19*, 3584–3588.
(19) Pierre, A. C. *Introduction to Sol-gel Processing*; Kluwer Academic: Boston, MA, 1998.

JA808092V